Nuclear Inst. and Methods in Physics Research, A 995 (2021) 165130

Contents lists available at ScienceDirect

Nuclear Inst. and Methods in Physics Research, A

journal homepage: www.elsevier.com/locate/nima

Low energy alpha particle tracks in CR-39 nuclear track detectors: Chemical etching studies

C.S. Oliveira [a], B. Malheiros [a,1], K.C.C. Pires [a,*], M. Assunção [b], S. Guedes [c], J.N. Corrêa [d], S.A. Paschuk [d]

[a] Departamento de Física Nuclear, Instituto de Física, Universidade de São Paulo, 05508-090, São Paulo, Brazil
[b] Departamento de Física, Universidade Federal de São Paulo, Campus Diadema, 09972-270, São Paulo, Brazil
[c] Instituto de Física Gleb Wataghin, Universidade Estadual de Campinas, 13083-859, São Paulo, Brazil
[d] Universidade Tecnológica Federal do Paraná, Campus Curitiba, 80230-901, Paraná, Brazil

ARTICLE INFO

Keywords:
CR-39 detector
Alpha particle
Nuclear track
Etch pit
Etching time
Bulk etching

ABSTRACT

The widely known CR-39 nuclear track detectors (NTDs) have been used to investigate the etch pits formed by alpha particles from a ^{241}Am source moderated to 1–2 MeV. The efficiencies of two available CR-39 plastic detectors, Lantrak and Baryotrak, have been studied as a function of the chemical etching time. The chemical etching solutions of the NaOH, KOH and NaOH+ethyl alcohol at 70 and 80°C have been applied to build etch pit diameter growths as well as density curves. The obtained growth curves of etch pit diameters have been compared under these different etching conditions, showing similar general trends for Baryotrak and Lantrak detectors for etching at 70°C. A slight divergence of the curves have been observed at 80°C for etching times above 400 min, revealing a small variation in the bulk etch rates between the two detector types. The etch pit density curves for both detectors have also been studied, showing a plateau for all etching conditions except for NaOH+ethyl alcohol at 80°C, in which there is a significant decrease in density after ≈ 600 min of etching. The results obtained with the protocols described in detail in this work show the pertinent precautions to be adopted in the chemical treatment of NTDs for the detection of alpha particle at low energies. In particular, the quantitative results highlight the limits of linear growth of pits and induction etching time for etch pits with diameters D=0 μm (EIT_0) and D=1 μm (EIT_1).

1. Introduction

Nuclear Track Detectors (NTDs) have been used to detect protons, antiprotons, alpha particles, fission fragments and a variety of swift heavy ions [1–3]. They have also been applied to fast and thermal neutron dosimetry [4–6] and to the characterization of alpha calibration sources [7]. The interaction of the particle with the detector molecular structure results in a modified cylindrical region along the particle trajectory (track). When applying chemical treatment, it is observed that the track etching rate (V_T) is larger than the bulk etching rate (V_B). Making use of an appropriate chemical etching, it is easy to obtain visible conical etch pits at the detector surface, which could be identified and counted using an optical microscope [8]. This radiation detection technique is quite employable due to its nice response, high sensitivity, reduced background, easy chemical treatment and low cost [2,3].

An interesting application of NTDs is the monitoring of environmental radon and its progeny, through the detection of alpha particles emitted by ^{222}Rn (5.5 MeV), ^{218}Po (6.0 MeV) and ^{214}Po (7.7 MeV). Poly-allyl diglycol carbonate (PADC) is the most used NTD for this purpose [9–14] and is commonly referred to as CR-39, which has a refractive index of 1.5, density of 1.32 g/cm^3 [15], and can be safely employed at temperatures up to 100°C [2]. For the purpose of radon monitoring PADC plates are placed inside diffusion chambers or are directly exposed in the air [8]. Etching response of CR-39 bombarded by alpha particles with energies varying up to 7.7 MeV has already been studied under specific etching conditions [16–19]. The purpose of the present investigation is to extend the etching studies (varying etching conditions) of pits produced by low energy alpha particles in CR-39 detectors.

The curves response of etch pit diameters, under different etching conditions in two different commercially available CR-39 materials irradiated with low energy alpha particles, are compared and analysed. The procedures for exposing the detectors to an ^{241}Am alpha source, chemical etching and reading of detectors are presented in Section 2.

* Corresponding author.
E-mail address: kelly@if.usp.br (K.C.C. Pires).
[1] Present address: Institute for Complex Molecular Systems, Department of Chemical Engineering and Chemistry, Eindhoven University of Technology, Eindhoven, The Netherlands.

https://doi.org/10.1016/j.nima.2021.165130
Received 14 September 2020; Received in revised form 23 December 2020; Accepted 6 February 2021
Available online 11 February 2021
0168-9002/

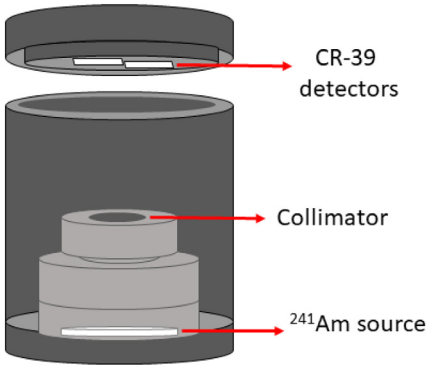

Fig. 1. Schematic diagram of the irradiation geometry inside of the lead castle.

In Section 3, the results obtained in the follow-up of the diameter and density etch pits are shown. In that same section, the curves obtained in these studies are analysed and discussed. Concluding remarks are presented in Section 4.

2. Materials and methods

Etching experiments have been carried out using two different types of CR-39 detectors, Lantrak and Baryotrak, manufactured by Fukuvi Chemical Industry Co LTD and sold by Landauer. The detectors have been exposed to alpha particles (E_α=5.486 MeV) from a thin planar radioactive ^{241}Am source for 6.5 h. This source has been produced by the Energy and Nuclear Research Institute (IPEN) of the National Nuclear Energy Commission (CNEN), Brazil, and has the activity of 1000 alpha particles/s. The CR-39 exposure has been performed using a collimator installed between the alpha source and the detectors, in order to reduce the track density and the alpha particle angle of incidence. In addition, the detectors have been displaced with respect to the axis of the source and the collimator positioning, which further reduced the number of tracks and their density, ensuring a larger room between two or more tracks, allowing a better size monitoring throughout the procedure. The distance between the ^{241}Am source and the plastic detectors has been kept fixed (41.36 mm) in all experiments. The ^{241}Am alpha source has been placed at the bottom of a lead castle while the CR-39 detectors have been attached to its lead cover (see Fig. 1), which has been tightly closed during the exposure.

To estimate the incidence energy of the alpha particles, two pieces of PADC have been exposed to an ^{241}Am source during the same interval of time of 6.5 h. In this procedure, an irradiation setup similar to that of Fig. 1 has been used, ensuring two different source-detector distances: 29.15 ± 0.46 mm and 41.36 ± 0.18 mm. Although etching experiments have been performed using only detectors exposed at a distance of 41.36 mm, studying the characteristics of etch pits formed around alpha particle tracks with different energies shall provide valuable comparative information. Exposed detectors have been etched together in a 6.25M NaOH solution for 400 min at 70 °C. Diameters of fifty round etch pits have been measured, for each detector, using a Zeiss Axioplan II microscope with nominal magnification of 1250×. A calibrated rule on one of the microscope eyepieces has been used to carry out the diameter measurements. The average etch pit diameter for the detectors exposed at a distance of 41.36 mm has been determined to be 9.1±0.4 μm. The etch pit diameters in the detector exposed at a distance of 29.15 mm have presented a mean value of 10.3±0.4 μm. Despite the similarity of mean diameter values, the etch pits in the detector exposed at 29.15 mm are darker than the etch pits in the detector exposed at 41.36 mm from the source, which suggests that alpha particle energies are above 2.0–2.5 MeV in the former, while alpha particles detected in the latter are in a range of energies below 2.0–2.5 MeV [16,20].

In Ref. [16], etch pitch diameters have been studied as a function of incident alpha particle energies. Since, in this work, the estimated values of alpha particle energies are roughly the same as those in Ref. [16], we have decided to follow the chemical etching protocol in that reference. For the two distances used for the exposure of the detectors (41.36 mm and 29.15 mm), the quadratic values of the diameters have been obtained as 83±8μm^2 and 107±9μm^2, respectively, to enable the comparison with the reference data [16], presented as products of diameters of round etch pits.

Under these conditions and considering the experimental uncertainties, the energy intervals of the incident alpha particles have been obtained in the range of 1–2 MeV (at the largest distance from the source) and 4–5 MeV (at the smaller distance from the source). The methodology used in this work enabled an estimate of the incident energy value as 1.5 ± 0.5 MeV.

Etching experiments have been carried out using three different chemical solutions: KOH (30% in mass); NaOH (6.25M); NaOH (6.25M) + ethyl alcohol (2%). KOH and NaOH solutions have been selected because they are the most common in different surveys involving PADC [3,8,13]. The addition of the ethyl alcohol in the NaOH solution is expected to reduce the sensitivity of the CR-39 to the etching process [21]. An increase in the V_b parameter has been observed for NaOH+ethanol solutions with different concentrations [22–24].

The detectors have been immersed in the etchant solution and maintained at a stable temperature of either 70°C or 80°C during the etching procedure. The chemical treatment has been performed gradually with etching time interval increment of 30 min, submitting repeatedly the same detector to chemical treatment using the same solution at the given temperature. After each step, the CR-39 detectors have been transferred to an acetic acid solution (CH_3COOH) to stop the etching process. Then they were washed in distilled water and stored. The chemical solutions have been prepared beforehand of each etching step [25–27].

Etch pits have been identified and visualized using a Leitz Diaplan optical microscope with magnification of 78.75×. At the central region of each CR-39 piece, areas for monitoring of etch pits growth in the etching experiments have been previously selected. With this purpose, a metallic screen has been used to ensure the same position of the detectors at the microscope table. Edge regions of CR-39 have been excluded from the measurements [28]. The same set of etch pits has been measured at each step of the successive etching procedures up to ≈ 12 h for KOH and NaOH solutions and up to ≈ 20 h for NaOH + ethyl alcohol solution. Only etch pits (with the ratio between the minor and major pit diameters bigger than 0.7) formed by nearly perpendicularly incident alpha particle tracks have been selected for the analysis of etch pit growth, performed by the software ImageJ [29]. Some examples of the etch pit evolution obtained using KOH solution at 80°C and NaOH + ethyl alcohol) solution at 70°C are shown in Fig. 2. Superficial densities of etch pits have also been determined after every etching experiment.

3. Results and discussions

3.1. Etch pit diameters

In Fig. 3, etch pit diameters (D) are shown as functions of the etching time for both Lantrak and Baryotrak CR-39 detectors. The presented values are the averages of etch pit diameters counted over the selected regions of the detector. The etch pit diameters have been measured immediately after each etching experiment. The uncertainties shown correspond to the average deviation. The etch pit diameters exhibit a gradual growth with a tendency to saturation with the increase of the etching time for different temperatures and chemical solutions.

For the etching carried out at 70°C, the etch pit diameters follow the same growth trend in both Lantrak and Baryotrak CR-39 detectors. For the etching at 80°C, the etch pit diameters for both types of detectors

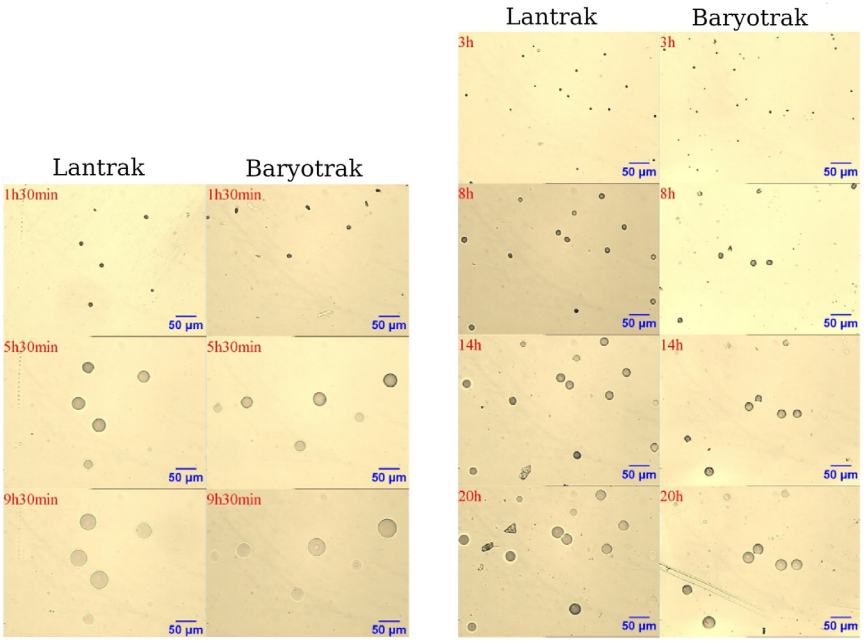

Fig. 2. Image examples of chosen regions of the CR-39 detectors etched with (left) KOH at 80°C and (right) NaOH + ethyl alcohol solutions at 70°C at different etching time steps.

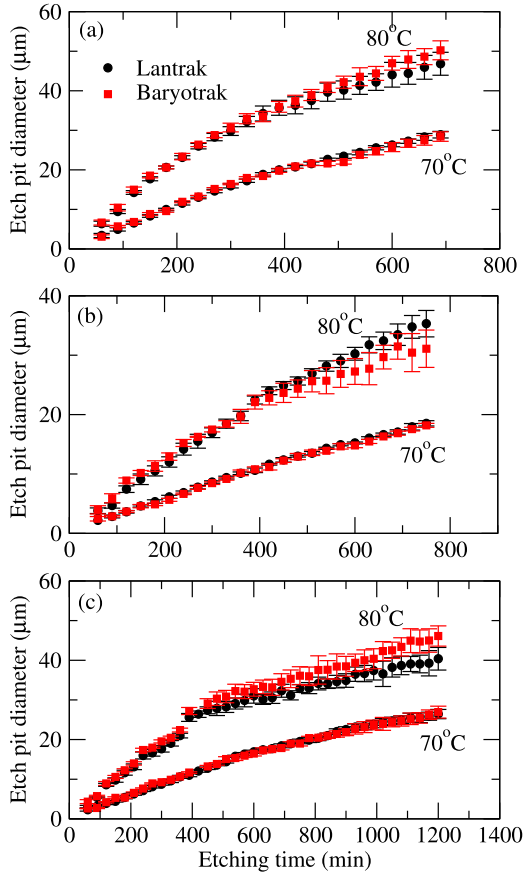

Fig. 3. Etch pit diameters versus etching time for Lantrak and Baryotrak CR-39 detectors using (a) KOH, (b) NaOH and (c) NaOH + ethyl alcohol solutions at 70°C and 80°C.

follow the same trend for etching times shorter than ≈ 400 min. For longer times, the growth curves split into different branches.

After overetching is reached, the etch pit diameters grow at a slower rate in the Lantrak detector for etching with KOH or NaOH+ethyl alcohol at 80°C. For the Baryotrak detector, the etch pit diameters present a slower growth for etching with NaOH solution. To summarize, the obtained results indicate that the V_T/V_b is close to the same ratio for the lower energy of alpha particles in Lantrak and Baryotrak detectors, but the corresponding bulk etching ratios are different.

No significant difference has been observed, which has then been both approximated to the time at the point of slope change. Even in the linear part of the etch pit growth curve, at 80°C the growth rate is about 50% higher as compared to the detectors etched at 70 °C, independently of the used chemical etchant. This result for alpha particles with ≈ 1.5 MeV is consistent with those found for 4.5 MeV alpha particles detected by the PADC in a study concerning counting efficiency variation with respect to etching temperature [30]. The referred study has been performed using NaOH (6.25M) as a chemical etchant. For etching performed at 80°C, it has been observed that the etch pit diameters presented a maximum size of 50 μm for a KOH solution at 650 min of etching time, in contrast to the etching with NaOH and NaOH + ethyl alcohol solution when etch pit diameters did not exceed 40 μm after the same etching time. A saturation in the growth rate of the etch pit diameter as a function of the etching time has been observed.

A direct comparison of the growth curves for the etch pit diameter obtained with NaOH and NaOH+ethyl alcohol solutions are shown in Fig. 4. There is no deviation of growth curves for the etching solutions at 70°C. For chemical etching at 80°C, differences are observed only for times longer than ≈ 400 min, indicating a small variation in V_b caused by the addition of ethyl alcohol, as previously observed in [24].

In order to find the time limit which establishes the curve deviation from linearity, we have adopted the procedure of adding one point at a time, observing the quadratic regression coefficient R^2 of the linear fitting. Thus, the final criterion to define this initial linear region is the best value of R^2. The growth rate of the etch pit diameter, dD/dt, is obtained directly from the data fitting. In Table 1, those results are shown.

The etching curves of Fig. 3 also allow the calculation of etch induction times (EIT). EIT has been defined as the etching time necessary to open the etch pit (D=0 μm), EIT_0 [31], or alternatively, as the

Table 1
Growth rate of the etch pit diameters dD/dt (in μm/h), for the Lantrak (L) and Baryotrak (B) detectors, limit times t_{lim} (in min), and regression coefficient R^2.

Chemical etchant	T °C	$^{L}[t_{lim}]$	$^{L}[R^2]$	^{L}[dD/dt]	$^{B}[t_{lim}]$	$^{B}[R^2]$	^{B}[dD/dt]
KOH	80	150	0.993	7.8	270	0.987	6.2
NaOH	80	450	0.997	3.3	300	0.987	3.3
NaOH + ethyl alcohol	80	450	0.987	3.6	300	0.989	3.9
KOH	70	270	0.999	3.2	330	0.995	3.2
NaOH	70	360	0.999	1.6	510	0.997	1.5
NaOH + ethyl alcohol	70	510	0.999	1.6	540	0.995	1.7

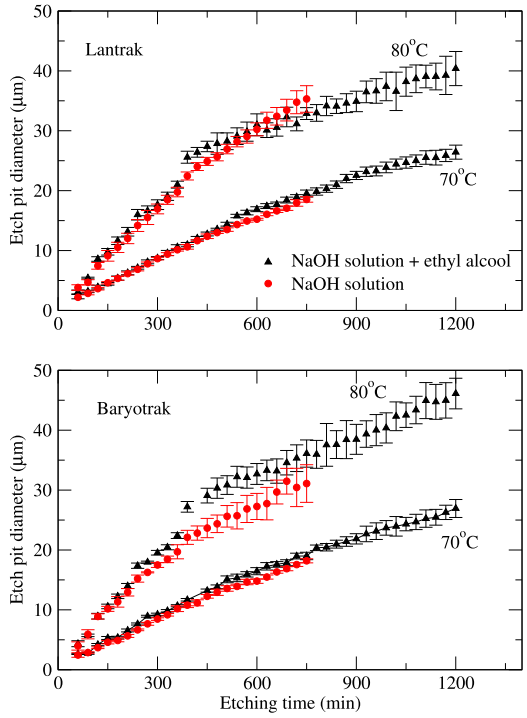

Fig. 4. Time evolution of etch pit diameters obtained with NaOH and NaOH + ethyl alcohol solutions for Lantrak and Baryotrak detectors at 70°C and 80°C.

time needed to grow the etch pit diameter at D=1 μm, EIT_1 [32]. To calculate the EIT values, the etching curves have been extrapolated through a linear approximation. EIT_0 is the point at which the curve crosses the etching time axis and EIT_1 is calculated from the linear extrapolation. As previously mentioned, in this work, the method to define the best extrapolation is the addition of experimental results, one by one, starting from the shorter etching time and going to the time limits, which are shown in Table 1.

The values of EIT_0 and EIT_1 are shown in Table 2. For EIT_0, only the Lantrak detector etched with KOH at 80°C resulted in a positive value. In this work, all data obtained for EIT_1 are in the range from 0 to 20 min approximately.

In Ref. [31], EIT values from previously published data are compiled. Alpha particles in the range of 0.23–1.3 MeV/u resulted in EIT_1 = 58–74 min, considering uncertainties [31,32]. This value is obtained for 6.0M NaOH etching solution at 70°C. Also, figure 5 of the referred paper presents the EIT as a function of Z/β, where β is given by the ratio of particle to light speeds. In our work, the energy per nucleon of alpha particles is 0.4±0.1 MeV/u, corresponding to a Z/β value of (70±20). The closer etching condition used, compared to Ref. [31], is 6.25M NaOH at 70°C. For this etching protocol, we have obtained EIT_1 = 18.6 min, a value smaller than those presented in Refs [31,32]. These deviations can be partially explained by the higher etchant concentration used in Ref. [31], which provides a more aggressive etching. Within the surface-cap segment model [31], this means a faster removal of track cap.

3.2. Superficial densities of etch pits

In Fig. 5, the curves of mean superficial densities of etch pits are shown. The experimental array and the procedure used for the chemical etching of the detectors intend to control a spacing between etch pits, large enough to an adequate measurement of the etch pit diameters. Etch pits of the same detector region have been measured and counted (see Fig. 2). Under this condition, the use of the Poisson counting uncertainty to compare the numbers of etch pits at different etching stages appears to be inappropriate. For this reason, the errors in the counting of the etch pits have been neglected in the calculation of the pit densities uncertainty.

The areas of the regions, on which etch pits have been counted and measured, have been kept constant during all experiments (see Fig. 2). Hence, the uncertainties in the etch pit densities have been estimated as 8%, considering only the systematic uncertainties concerning the area determination.

The etch pit densities increase rapidly, becoming constant during the etching process. In particular, the detectors etched at 80°C present shorter saturation times as compared to those of the detectors etched at 70°C (see Table 3). The stabilization of the etch pit diameters occurs long after the etch pit diameters have reached the plateau levels (compare Figs. 3 and 5). This rapid density uniformity is a consequence of the nearly perpendicular incidence of alpha particles from the external sources onto the detectors inside the irradiation setup. As all tracks originate inside the etched surface, no new track will appear when the surface layers are removed. Worth of notice is the remarkable decrease in etch pit density in the detectors etched at 80°C with NaOH + ethyl alcohol, starting after 900 min of etching. This response may be a consequence of adding ethyl alcohol to the NaOH solution, which manifests only for longer etching times in the more aggressive temperature of 80°C [27]. A perceptible increase in the bulk etching rate, which results in a reduction of the detection efficiency, has been observed under less extreme etching conditions but for ethanol concentrations at least 5 times higher than that employed in this work [24].

3.3. Choice of etching protocols

The etch pit diameter growth rate and density curves obtained in the present work may be useful to find out the best etching condition for the intended application. For instance, the monitoring of low levels of Radon, in which low densities of alpha particles are usually obtained, may be better analysed after the etching process producing larger etch pits. These large etch pits could be seen at lower microscope magnifications, in such a way that extensive detector areas can be scanned more rapidly. From Fig. 3, it is clear that the KOH etchant will produce the larger etch pits. On the other hand, in applications to produce higher track densities, as the detection of alpha particle tracks in thermal neutron monitoring using boron converters [4], the detectors will be better analysed if they produce smaller etch pits after the etching process. In this case, NaOH may be more suitable in the etchant solution. In addition, the chosen etching protocol must be robust enough to avoid changes in etch pit densities due to small variations of etching conditions, mainly temperature. An analysis of Fig. 5 may help us in this discussion. The KOH etching yields reproducible

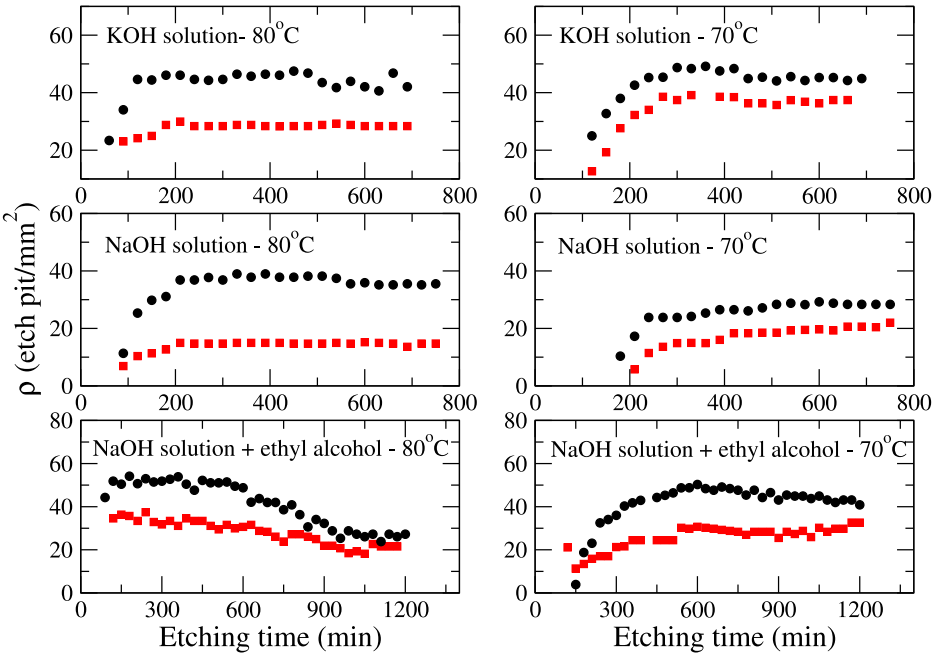

Fig. 5. Etch pit densities of the Lantrak (black circles) and Baryotrak (red squares) detectors etched with the KOH (top), NaOH (middle) and NaOH + ethyl alcohol (bottom) solution versus etching time.

Table 2
The obtained values of the induction etching times for the etch pits with diameters D=0 μm (EIT_0) and D=1 μm (EIT_1). Negative EIT values are marked as neg. Results are presented for the Lantrak (L) and Baryotrak (B) detectors.

Chemical etchant	T (°C)	$^{L}[EIT_1]$(min)	$^{L}[EIT_0]$(min)	$^{B}[EIT_1]$(min)	$^{B}[EIT_0]$(min)
KOH	80	20.4	12.7	neg	neg
NaOH	80	8.8	neg	neg	neg
NaOH + ethyl alcohol	80	11.3	neg	7.2	neg
KOH	70	15.4	neg	11.3	neg
NaOH	70	18.6	neg	14.6	neg
NaOH + ethyl alcohol	70	13.5	neg	5.0	neg

Table 3
Uniform values of pit density and stabilization time, t_s, for Lantrak (L) and Baryotrak (B) detectors corroded with KOH, NaOH and (NaOH+ethyl alcohol) etchants at 70°C and 80°C. Etch pit densities, ρ is given in etch pit/mm^2.

Chemical etchant	T °C	$^{L}[t_s$(min)]	$^{L}[\rho]$	$^{B}[t_s$(min)]	$^{B}[\rho]$
KOH	80	210	46.07	150	24.96
NaOH	80	210	36.85	180	12.67
NaOH + ethyl alcohol	80	120	51.82	120	34.55
KOH	70	270	45.37	150	19.28
NaOH	70	240	23.82	240	11.46
NaOH + ethyl alcohol	70	390	42.93	330	21.59

densities from approximately 400 min for etching at 70°C, and 300 min for etching at 80°C. Therefore, an etching time of 400 min or longer would be more feasible. The same analysis for the NaOH etchant will lead to similar conclusions. On the other hand, the NaOH+ethyl alcohol solution seems to present no range of etching duration on which the etching process produces stability simultaneously for the temperatures of 70°C and 80°C.

4. Conclusions

The efficiencies of two types of PADC detectors, Lantrak and Baryotrak, for the detection of alpha particles in the range of ≈ 1–2 MeV, have been studied as a function of the chemical etching time by using three chemical solutions: KOH, NaOH and NaOH + ethyl alcohol at two different temperatures, 70°C and 80°C. For both temperatures, the etch pits of alpha particles evolved in a similar manner to relatively high energy alpha particle tracks [33].

In a previous publication [33], a pit diameter growth rate of 1.8 μm/h has been obtained for a track etching of 3.1 MeV alpha particle in CR-39 using NaOH 6.25M at 70°C. This value is in agreement with our measurements under the same etching conditions. Our results also indicate that a small variation of etchant concentration will have a non-negligible impact on the onset of etch pit formation, quantified by the etch induction time.

For all practical purposes, there is no important efficiency difference between Lantrak and Baryotrak detectors for the detection of low energy alpha particles. Also, the addition of ethyl alcohol into the NaOH solution has not improved the efficiency gain, although it has provided a visual improvement in the sharpness of pits observed under the microscope for detectors exposed for long etching times.

The monitoring of the pits diameter has allowed the calculation of its growth rate, dD/dt, by considering the limit of the time of chemical etching for the different temperatures and chemical solutions to which the Lantrak and Baryotrak NTDs have been submitted. In this work, the values of limiting times stand around 300 min for Baryotrak detectors etched at 80°C and, around 500 min for those etched at 70°C, except for the ones revealed in the KOH solution whose limiting times remain around 300 min. In the case of Lantrak, the values ranged from 150 to 450 min at T = 80°C and in the range from 270 to 510 min at T = 70°C. Also, in the quantitative analysis, the values of the time of the induction etching times for the etch pits have been determined with diameters of the D=0 μm (EIT_0) and D=1 μm (EIT_1) (see Table 2).

The etch pit size and density growth curves presented here constitute a comprehensive dataset that can be useful in further CR-39 applications. The choice of the best etchant depends on the intended application. A general feature brought about by our results is that NaOH seems to be better suited for applications involving larger track densities, while KOH is recommended for applications involving smaller track densities.

CRediT authorship contribution statement

C.S. Oliveira: Methodology, Formal analysis, Investigation. **B. Malheiros:** Methodology, Formal analysis, Investigation, Writing - original draft, Writing - review & editing. **K.C.C. Pires:** Conceptualization, Validation, Formal analysis, Data curation, Writing - original draft, Writing - review & editing, Supervision, Project administration. **M. Assunção:** Validation, Formal analysis, Data curation, Writing - original draft, Writing - review & editing. **S. Guedes:** Validation, Formal analysis, Investigation, Resources, Writing - review & editing. **J.N. Corrêa:** Methodology, Resources. **S.A. Paschuk:** Resources, Writing - review & editing.

Declaration of competing interest

The authors declare that they have no known competing financial interests or personal relationships that could have appeared to influence the work reported in this paper.

Acknowledgements

The authors would like to thank the Conselho Nacional de Desenvolvimento Científico e Tecnológico (CNPq/MCTI), Brazil grants #100734/2015-4 and #308192/2019-2, São Paulo Research Foundation (FAPESP) grant #2019/07767-1, and the University of São Paulo, Brazil for the financial support. The authors are grateful to F. E. M. Silveira for comments and suggestions.

References

[1] C. Baccou, V. Yahia, S. Depierreux, C. Neuville, C. Goyon, F. Consoli, R. De Angelis, J.E. Ducret, G. Boutoux, J. Rafelski, C. Labaune, CR-39 track detector calibration for H, He, and C ions from 0.1-0.5 MeV up to 5 MeV for laser-induced nuclear fusion product identification, Rev. Sci. Instrum. 86 (2015) 083307, http://dx.doi.org/10.1063/1.4927684.

[2] M.A. Rana, Thermodynamics of nuclear track chemical etching, Nucl. Instrum. Methods Phys. Res. A 890 (2018) 68–71, http://dx.doi.org/10.1016/j.nima.2018.02.041.

[3] M.A. Rana, Summary of a comprehensive data bank for nuclear track research using CR-39 detectors, Nucl. Instrum. Methods Phys. Res. A, 944 (2019) 162590, http://dx.doi.org/10.1016/j.nima.2019.162590.

[4] B. Smilgys, S. Guedes, M. Morales, F. Alvarez, J.C. Hadler, P.R.P. Coelho, P.T.D. Siqueira, I. Alencar, C.J. Soares, E.A.C. Curvo, Boron thin films and CR-39 detectors in BNCT: A method to measure the $^{10}B(n,\alpha)^{7}Li$ reaction rate, Radiat. Meas. 50 (2013) 181–186, http://dx.doi.org/10.1016/j.radmeas.2012.07.001.

[5] F. Assenmacher, M. Boschung, E. Hohmann, S. Mayer, Comparison of different PADC materials and etching conditions for fast neutron dosimetry, Radiat. Prot. Dosim. 170 (1-4) (2016) 162–167, http://dx.doi.org/10.1093/rpd/ncv421.

[6] R. Kwiatkowski, A. Malinowska, M. Gierlik, J. Rzadkiewicz, A. Szydlowski, A. Urban, K. Mikszuta, Assessment of 14 MeV DT neutron generator emission with activation and particle track methods, Fusion Eng. Des. 146 (2019) 1060–1063, http://dx.doi.org/10.1016/j.fusengdes.2019.02.002.

[7] E. Segreto, A.A. Machado, L. Paulucci, F. Marinho, D. Galante, S. Guedes, A. Fauth, V. Teixeira, B. Gelli, M.R. Guzzo, W. Araujo, C. Ambrósio, M. Bissiano, A.L. Lixandrão Filho, Liquid argon test of the ARAPUCA device, J. Instrum. 13 (2018) P08021, http://dx.doi.org/10.1088/1748-0221/13/08/P08021.

[8] D. Nikezic, K.N. Yu, Formation and growth of tracks in nuclear track materials, Mater. Sci. Eng. R 46 (3) (2004) 51–123, http://dx.doi.org/10.1016/j.mser.2004.07.003.

[9] M.E. Smith, O.A. Dumitru, B.D. Burghele, A. Cucos, B.P. Onac, Radon concentration in three Florida caves: Florida, Jennings, and Ocala, Carbonates and Evaporites 34 (2019) 433–439, http://dx.doi.org/10.1007/s13146-018-0473-7.

[10] K. Ivanova, Z. Stojanovska, B. Kunovska, N. Chobanova, V. Badulin, A. Benderev, Analysis of the spatial variation of indoor radon concentrations (national survey in Bulgaria), Environ. Sci. Pollut. Res. 26 (2019) 6971–6979, http://dx.doi.org/10.1007/s11356-019-04163-9.

[11] L. Tommasino, J. Chen, R. Falcomer, M. Janik, R. Kanda, F. DeFelice, F. Cardellini, R. Trevisi, F. Leonardi, M. Magnoni, E. Chiaberto, G. Agnesod, M. Faure Ragani, G. Espinosa, J. Golzarri, K. Kozak, J. Mazur, An international cooperation by using an all-encompassing passive radon monitor, Radiat. Prot. Dosim. 177 (1-2) (2017) 12–15, http://dx.doi.org/10.1093/rpd/ncx162.

[12] V. Zorri, R. Remetti, M. Capogni, G. Cotellessa, R. Falcone, Feasibility study on the application of solid state tracks detectors for fast surveys of residual alpha contamination in decommissioning activities, Radiat. Meas. 107 (2017) 111–114, http://dx.doi.org/10.1016/j.radmeas.2017.09.004.

[13] G. Espinosa, J.I. Golzarri, A. Angeles, R.V. Griffith, Nationwide survey of radon levels in indoor workplaces in Mexico using nuclear track methodology, Radiat. Meas. 44 (9) (2009) 1051–1054, http://dx.doi.org/10.1016/j.radmeas.2009.10.035.

[14] S.R. Paulo, R. Neman, J.C. Hadler, P.J. Iunes, S. Guedes, A.M.O.A. Balan, C.A.S. Tello, Radon surveys in Brazil using CR-39, Radiat. Meas. 39 (2005) 657–660, http://dx.doi.org/10.1016/j.radmeas.2004.06.017.

[15] Shi-Lun Guo, Bao-Liu Chen, S.A. Durrani, Chapter 3 - Solid-state nuclear track detectors, in: M.F. L'Annunziata (Ed.), Handbook of Radioactivity Analysis, Fourth ed., Academic Press, 2020, pp. 307–407.

[16] C.J. Soares, I. Alencar, S. Guedes, R.H. Takizawa, B. Smilgys, J.C. Hadler, Alpha spectrometry study on LR115 and Makrofol through measurements of track diameter, Radiat. Meas. 50 (2013) 246–248, http://dx.doi.org/10.1016/j.radmeas.2012.06.010.

[17] Y. Zhang, H.W. Wang, Y.G. Ma, L.X. Liu, X.G. Cao, G.T. Fan, G.Q. Zhang, D.Q. Fang, Energy calibration of a CR-39 nuclear-track detector irradiated by charged particles, Nucl. Sci. Tech. 30 (2019) 87, http://dx.doi.org/10.1007/s41365-019-0619-x.

[18] D. Hermsdorf, Evaluation of the sensitivity function V for registration of α-particles in PADC CR-39 solid state nuclear track detector material, Radiat. Meas. 44 (3) (2009) 283–288, http://dx.doi.org/10.1016/j.radmeas.2009.03.028.

[19] D. Hermsdorf, Physics aspects of light particle registration in PADC detectors of type CR-39, Radiat. Meas. 46 (4) (2011) 396–404, http://dx.doi.org/10.1016/j.radmeas.2011.02.012.

[20] J.C. Hadler, S.R. Paulo, Indoor radon daughter contamination monitoring - the absolute efficiency of CR-39 taking into account the plateout effect and environmental conditions, Radiat. Prot. Dosim. 51 (4) (1994) 283–296, http://dx.doi.org/10.1093/oxfordjournals.rpd.a082146.

[21] S.A. Durrani, R.K. Bull, Solid State Nuclear Track Detection: Principles, Methods, and Applications, Pergramon Press, 1987.

[22] Y.Y. Kasim, Bulk etch rate of CR-39 detector using NaOH/ethanol etchant, Jordan J. Phys. 10 (2017) 97–103, http://journals.yu.edu.jo/jjp/JJPIssues/Vol10No2pdf2017/3.pdf.

[23] K.F. Chan, F.M.F. Ng, D. Nikezic, K.N. Yu, Bulk and track etch properties of CR-39 SSNTD etched in NaOH/ethanol, Nucl. Instrum. Methods Phys. Res. B 263 (1) (2007) 284–289, http://dx.doi.org/10.1016/j.nimb.2007.04.148.

[24] E.M. Awad, M.A. Rana, Bulk etch rates of CR-39 nuclear track detectors over a wide range of etchant (NaOH aqueous solution+ethanol) concentrations: measurements and modeling, Radiat. Eff. Defects Solids 175 (11-12) (2020) 1109–1126, http://dx.doi.org/10.1080/10420150.2020.1810038.

[25] M.A. Rana, CR-39 nuclear track detector: an experimental guide, Nucl. Instrum. Methods Phys. Res. A 910 (2018) 121–126, http://dx.doi.org/10.1016/j.nima.2018.08.077.

[26] M.A. Rana, How to achieve precision and reliability in experiments using nuclear track detection technique? Nucl. Instrum. Methods Phys. Res. A 592 (3) (2008) 354–360, http://dx.doi.org/10.1016/j.nima.2008.04.025.

[27] D. Hermsdorf, Influence of external and internal conditions of detector sample treatment on the particle registration sensitivity of solid state nuclear track detectors of type CR-39, Radiat. Meas. 47 (7) (2012) 518–529, http://dx.doi.org/10.1016/j.radmeas.2012.05.002.

[28] Y.L. Law, D. Nikezic, K.N. Yu, Optical appearance of alpha-particle tracks in CR-39 SSNTDs, Radiat. Meas. 43 (2008) S128–S131, http://dx.doi.org/10.1016/j.radmeas.2008.03.030.

[29] Programme imagej, 2020, http://imagej.nih.gov/ij/index.html. (Accessed 08 December 2020).
[30] S. Guedes, J.C. Hadler, P.J. Iunes, S.R. Paulo, C.A. Tello, On the reproducibility of SSNTD track counting efficiency, Nucl. Instrum. Methods Phys. Res. A 418 (2) (1998) 429–433, http://dx.doi.org/10.1016/S0168-9002(98)00918-8.
[31] M.A. Rana, On the long standing question of nuclear track etch induction time: surface-cap model, Nucl. Instrum. Methods Phys. Res. B 266 (2) (2008) 271–276, http://dx.doi.org/10.1016/j.nimb.2007.10.036.
[32] H.A. Khan, T. Lund, P. Vater, R. Brandt, J.W.N. Tuyn, Some gross features of the interaction of semirelativistic ^{16}O and ^{12}C ions with ^{197}Au targets, Phys. Rev. C 28 (1983) 1630–1634, http://dx.doi.org/10.1103/PhysRevC.28.1630.
[33] N.F. Kadhum, L.A. Jebur, A.A. Ridha, Studying different etching methods using CR-39 nuclear track detector, Detection 4 (2016) 45–53, http://dx.doi.org/10.4236/detection.2016.43007.